Exploring the microbiome of healthy and diseased peri-implant sites using Illumina sequencing

Sanz-Martin, Ignacio ; Doolittle-Hall, Janet ; Teles, Ricardo P ; Patel, Michele ; Belibasakis, Georgios N ; Hämmerle, Christoph H F ; Jung, Ronald E ; Teles, Flavia R F

DOI: https://doi.org/10.1111/jcpe.12788

DR. IGNACIO SANZ MARTIN (Orcid ID : 0000-0001-7037-1163)

DR. RICARDO TELES (Orcid ID : 0000-0002-4216-2812)

DR. FLAVIA TELES (Orcid ID : 0000-0001-6945-9811)

Article type : Epidemiology (Cohort study or case-control study)

Exploring the microbiome of healthy and diseased peri-implant sites using Illumina Sequencing.

nz-Martin I[1], Doolittle-Hall J[2], Teles RP[3], Patel M[4], Belibasakis GN[5], Hämmerle CH[6], Jung [6], Teles FRF[3]

[1]Section of Periodontology, Faculty of Odontology, University Complutense of Madrid, Madrid, Spain.

[2]Department of Dental Ecology, University of North Carolina at Chapel Hill School of Dentistry, NC, USA.

[3]Department of Periodontology, University of North Carolina at Chapel Hill School of Dentistry, NC, USA.

[4]Department of Applied Oral Sciences, The Forsyth Institute, Cambridge, MA, USA.

[5]Department of Dental Medicine, Karolinska Institute, Stockholm, Sweden.

[6]Clinic of Fixed and Removable Prosthodontics and Dental Material Science, Center of Dental Medicine, University of Zürich, Switzerland.

Key words: microbiome; dental implant; peri-implantitis; DNA; periodontal; sequencing

Address for correspondence:

Flavia R. F. Teles
Department of Periodontology
UNC School of Dentistry
Koury Health Sciences Building
385 S. Columbia Street Room 3406
Chapel Hill, NC 27599-7455
fteles@email.unc.edu

ABSTRACT

Aim: To compare the microbiome of healthy (H) and diseased (P) peri-implant sites and determine the core peri-implant microbiome.

Materials and Methods: Submucosal biofilms from 32 H and 35 P sites were analyzed using 16S rRNA sequencing (MiSeq, Illumina), QIIME and HOMI*NGS*. Differences between groups were determined using Principal Coordinate Analysis (PCoA), t-tests and Wilcoxon rank sum test and FDR-adjusted. The peri-implant core microbiome was determined.

Results: PCoA showed partitioning between H and P at all taxonomic levels. *Bacteroidetes*, *Spirochetes* and *Synergistetes* were higher in P, while *Actinobacteria* prevailed in H ($p<0.05$). *Porphyromonas* and *Treponema* were more abundant in P and while *Rothia* and *Neisseria* were higher in H ($p<0.05$). The core peri-implant microbiome contained *Fusobacterium, Parvimonas* and *Campylobacter sp. T. denticola* and *P. gingivalis* levels were higher in P, as well as *F. alocis*, *F fastidiosum* and *T. maltophilum* ($p<0.05$).

Conclusion: The peri-implantitis microbiome is commensal-depleted and pathogen-enriched, harboring traditional and new pathogens. The core peri-implant microbiome harbors taxa from genera often associated with periodontal inflammation.

Clinical Relevance

Scientific rationale for study: there is a need for a better understanding of the microbial etiology of peri-implant diseases.

Principal findings: peri-implantitis sites were heavily colonized by well-known and newly proposed pathogens, including as-of-yet uncultivated taxa, while healthy peri-implant sites harbored more commensal taxa. The peri-implant core microbiome was enriched for *Fusobacterium, Parvimonas* and *Campylobacter* species.

Practical implications: Better characterization of the peri-implant microbiome can improve the understanding of the etiology of peri-implant diseases.

Conflict of Interest

Dr. Ignacio Sanz Martín received an ITI Scholarship from October 2010 to October 2011. The other authors report no conflict of interest.

Sources of Funding:

This study was supported in part by an ITI Scholarship (to I.S.M.), by the National Institutes of Health/National Institute of Dental and Craniofacial Research (R03-DE021742 and R01-DE024767 to F.R.F.T.) and by a pilot grant from Forsyth's Center for Discovery at the Host-Biofilm Interface (to F.R.F.T).

Introduction

The widespread use of implants has led to an increase in the number of cases of biofilm-mediated peri-implant diseases, particularly peri-implantitis. Although long-term longitudinal studies indicate that implant therapy presents success rates of 95% - 99% (Moraschini et al., 2015, Vigolo et al., 2015) recent publications have shown a prevalence of peri-implantitis of at least 20% (Derks et al., 2016b, Derks et al., 2016a, Derks & Tomasi, 2015, Mombelli et al., 2012, Derks & Tomasi, 2014). It has been suggested that peri-implantitis progresses in non-linear patterns, and for the majority of cases, the onset occurs within 3 years of function (Derks et al. 2016b). Peri-implantitis treatment is further complicated by the limited knowledge of its microbial etiology. While several studies have shown microbial similarities between periodontitis and peri-implantitis (Carcuac et al., 2016, Charalampakis & Belibasakis, 2015, Mombelli & Decaillet, 2011), others have implicated species not traditionally associated with periodontal/peri-implant diseases, such as *Helicobacter pylori, Haemophilus influenzae, Staphylococcus aureus* and *Staphylococcus anaerobius* in the etiology of peri-implantitis (Persson & Renvert 2014). The current poor understanding of the microbial etiology and pathogenesis of peri-implantitis may help explain the lack of effective treatment.

Most of the publications that investigated the microbial profiles of peri-implantitis employed close-ended molecular approaches, which preclude the identification of potentially relevant taxa that are not targeted by the technique. The use of 16S rRNA Illumina sequencing can overcome this limitation by allowing an open-ended characterization of the microbiome under study (Caporaso et al., 2012, Frey et al., 2014, Smith & Peay, 2014), at a coverage depth 100 times greater than pyrosequencing, with a lower error rate and generating well over 10 times as many

reads as 454 GS FLX (Nelson et al., 2014). Because it combines higher sequence quality at significantly lower cost per sequence, it has become the leading sequencing platform for human microbiome sequencing studies (Amarasekara et al., 2015). One limitation of 16S rRNA sequencing is that certain taxa cannot be distinguished with species-level taxonomic resolution when the commonly employed QIIME pipeline is used for the downstream taxonomic classification (Baker et al., 2003, Chakravorty et al., 2007, Ong et al., 2013, Pei et al., 2010, Wang & Qian, 2009). To manage this limitation, we analyzed the reads generated by MiSeq with HOMI*NGS* in order to obtain species-level data. HOMI*NGS* is an *in silico* probe-based platform that can detect more than 600 bacterial species from 16S rRNA reads (Belstrom et al., 2016a).

The objective of the present investigation was to compare the microbiome of healthy (H) and diseased (P) peri-implant sites using 16S rRNA Illumina sequencing and HOMI*NGS* and to determine the peri-implant core microbiome.

Materials and Methods

Patient recruitment

This study was approved by the Ethical Review Committee of the Canton of Zürich, Switzerland (KEK-Nr: 2011-0159), and was conducted in accordance with the guidelines of the world Medical Association Declaration of Helsinki. Peri-implantitis patients were recruited as outpatients referred by private practitioners for the diagnosis and treatment of peri-implant disease at the Interdisciplinary Peri-implantitis Unit, in the Center of Dental Medicine at the University of Zürich. Patients presenting successful implants were recruited from the maintenance clinic at the same institution. Potential participants were informed about the aims of the study and were assured that their participation was voluntary. All participants provided

written informed consent. The inclusion criteria were good medical health as evidenced by the medical history, being at least 18 years old and willing to participate in the study. Exclusion criteria were as follows: periodontal or peri-implant treatment within the past 12 months, systemic antibiotics use within the past 6 months, pregnancy or lactation, and heavy smoking (>20 cigarettes/day).

Patients allocated to the peri-implantitis group presented at least one implant with post-insertion (i.e. at least one-year after loading) radiographic marginal bone loss of at least 2.0 mm mesially or distally, with concomitant bleeding on probing, according to the definitions presented in the European Workshop on Periodontology (Zitzmann & Berglundh, 2008). Radiographic bone levels were recorded by measuring the distance from the implant shoulder to the first visible bone to implant contact at the mesial and distal aspect of each implant using periapical radiographs.

The successful implants group included implants with healthy surrounding soft and hard tissues, determined by absence of pus and detectable radiographic bone loss, and functional loading for at least one year. Gender and age were recorded, as well as plaque index (PI), bleeding on probing (BOP), suppuration (SUP), probing pocket depth (PPD), clinical bone loss (BL in mm), width of keratinized mucosa (KM), implant wear time, time since last check up, implant system used and nature of reconstruction (single implant, fixed or removable). The clinical parameters were measured at 6 sites per implant (mesio-, mid-, disto-buccal and mesio-, mid-, disto-lingual/palatal; except for KM, where the palatal sites were not measured).

Submucosal biofilm sample collection and nucleic acid isolation

Submucosal biofilm samples were collected from peri-implantitis sites (P) in peri-implantitis patients and from healthy peri-implant sites (H) of participants presenting successful implants. If multiple implants were present in a patient, one single implant was randomly selected for sampling. Samples were obtained from the site with the deepest PPD. Prior to sampling, the supramucosal areas of the implant and supra-structure were isolated using cotton rolls, air-dried and had the supramucosal biofilm removed. Submucosal biofilm samples were obtained with sterile Gracey curettes (Deppeler, Rolle, Switzerland). The sample was immediately placed in a micro-centrifuge tube containing 0.1 ml of RNAse-free TE buffer (10 mM Tris-HCl, 1 mM EDTA, pH 7.6) and stored at -80°C until analysis.

Bacterial nucleic acids were isolated using the Masterpure DNA purification kit (Epicentre, Madison, WI, USA), preceded by an overnight incubation with lysozyme at 37°C. DNA quality and amount were determined using a spectrophotometer and the Picogreen dsDNA quantification assay (Invitrogen, Carlsbad, CA, USA).

16S rRNA gene sequencing with Illumina sequencing

Sample DNA was analyzed by sequencing the 16S rRNA gene V3-V4 hypervariable region using MiSeq (Illumina, CA), according to the protocol described by (Caporaso et al., 2011). In brief, 10-50 ng of DNA were PCR-amplified using the 341F/806R universal primers targeting the V3-V4 hypervariable region: 341F (forward) AATGATACGGCGACCACCGAGATCTACACTATGGTAATTGTCCTACGGGAGGCAGC AG; 806R (reverse) CAAGCAGAAGACGGCATACGAGAT**TCCCTTGTCTCC** AGTCAGTCAGCCGGACTACHVGGGTWTCTAAT, where the 'TCCCTTGTCTCC' region

represents the appropriate barcode sequences and the underlined bases make the PCR products Illumina sequencing compatible. PCR samples were purified using AMPure beads and 100 ng of each barcoded library were pooled, purified and quantified using a bioanalyzer and qPCR. Then, 12 pM of each library mixture spiked with 20% PhiX was loaded onto the MiSeq and sequenced. Samples that presented poor performance in the pre-sequencing PCR amplification step were amplified by multiple displacement amplification (Teles et al., 2007) using the Illustra GenomiPhi V2 DNA Amplification kit (GE Healthcare, USA). Quality control of the reads was performed using FastQC. The paired end reads were merged using Flash.

Taxonomic assignment

The reads generated using MiSeq were analyzed using the QIIME pipeline (Caporaso et al. 2010). In brief, the paired-end reads were merged using Flash. The libraries were split in QIIME according to the barcodes used in the sequencing run and low-quality reads were filtered out and chimeras were removed using UCHIME. Operational taxonomic units (OTUs) were picked using the Human Oral Microbiome Database (HOMD) v13.2 as the reference database (Chen et al. 2010) using a 97% similarity threshold. Taxonomy was assigned using the Ribosomal Database Project (RDP) classifier trained on the HOMD v13.2 database with assignments required to meet a >80% confidence threshold. The phylum and genus-level analyses were performed using QIIME.

For species-level analyses only, we employed HOMI*NGS*, an *in silico* 16S rDNA probe analysis that allows for species-level identification of sequencing datasets generated with MiSeq (http://homings.forsyth.org) (Gomes et al., 2015). Species-specific, 16S rRNA-based oligonucleotide “probes” were used in a Perl program based on text string search to identify the

frequency of oral bacterial targets. HOMI*NGS* comprises 671 oligonucleotide probes of 17 to 40 bases that target 538 individual oral bacterial species/phylotypes or, in some cases, a few closely-related taxa. (Belstrom et al., 2016a, Belstrom et al., 2016d).

Statistical analysis

The demographic and clinical characteristics of the study population were analyzed using the Fisher's Exact Test or Student's t-test. Effects of disease status on the peri-implant microbiome were examined using Principal Coordinate Analysis (PCoA).

Significant differences in relative abundance (%) between the clinical groups were determined at the phylum, genus, and species levels. Raw read counts were rarefied to the minimum number of aligned reads. Only taxa that had at least 3 reads in at least 3 samples in both clinical groups after rarefication were considered. Significant differences between the healthy and peri-implantitis groups were determined by Wilcoxon rank sum test with FDR-adjusted p-values <0.05. This rarefication and determination of significance was repeated 100 times. Taxa that were significant in 95% of these iterations were further considered in the analyses. Interactions between those taxa and smoking, as well as implant type were assessed using ANOVA.

The core microbiome of the dataset was determined based on taxa present with $\geq 0.1\%$ relative abundance in $\geq 50\%$ of all samples, as determined by HOMI*NGS* (Abusleme et al., 2013). It was subdivided into 4 groups based on the taxa mean relative abundance in samples in each clinical category. Taxa that were present in $\geq 50\%$ of samples in either the H or P groups, but were not part of the core microbiome considering all samples, constituted the healthy or peri-implantitis core microbiomes, respectively.

Results

Demographic and clinical characteristics of the subjects

Eighty-two patients contributing with one implant per patient were initially included in the investigation. Fifteen patients were excluded due to issues with microbial sampling. Finally, the analysis of demographic and clinical data from the sampled population showed that the groups comprising healthy (H, N=32) and diseased peri-implant sites (P, N=35) were well-balanced for age, gender, implant wear, implant location and type of restoration (Table 1). Non-smokers and smokers comprised 37.1% and 42.9% of the P group, respectively, whereas in the H group these were 71.9% and 21.9%, respectively ($p=0.03$). Straumann was the most frequently used implant system in both groups (71.9% in H and 47.1% in P), while other systems (i.e., not Straumann or Branemark) were more common in P (35.3%) than in H (3.1%) ($p=0.003$). Significant differences between the groups were observed for the clinical parameters that defined them ($p<0.0001$).

Overall microbial sequencing results

Fifteen samples (7 in disease, 8 in health) were excluded from analysis due to the small number of reads (<5,000). After quality control, chimera depletion and noise filtering, 7,297,772 reads (median/sample: 114,230; range: 5,055-212,299) were assigned into OTUs (1.7% of them remained unassigned) and most of them (73.52%) ranged from 408 to 428 bp in length. OTUs were classified into twelve phyla: *Bacteroidetes* (25.3%), *Proteobacteria* (18.4%), *Firmicutes* (16.7%), *Actinobacteria* (15.6%), *Fusobacteria* (15.6%), *Spirochaetes* (5.3%), *Synergistetes*

(0.7%), *Tenericutes* (0.4%), *TM7* (0.3%), SR1 (0.1%), *Chloroflexi* (0.01%) and GN02 (0.001%). These OTUs were further classified into 21 classes, 35 orders, 69 families and 94 genera, using QIIME. HOMI*NGS* identified 85 genera and 210 species using species-specific "probes". A complete list of species detected in H and P samples can be found in Supplemental Table 1.

Microbial profiles of healthy and diseased peri-implant sites

Diseased peri-implant sites presented higher diversity, compared to healthy sites (Supplemental Fig. 1a). Healthy (H) and diseased (P) peri-implant sites presented distinct microbial profiles at all taxonomic levels (Fig. 1a-c, Supplemental Fig. 1b). Diseased peri-implant sites were primarily colonized by members of the phyla *Bacteroides*, *Spirochetes* and *Synergistetes*, whereas healthy peri-implant sites mostly harbored taxa from the *Proteobacteria* and *Actinobacteria* phyla ($p<0.05$, FDR-adjusted) (Fig. 1a). The genera *Porphyromonas* (phylum *Bacteroidetes), Treponema* (phylum *Spirochetes*), *Filifactor* (phylum *Firmicutes), Fretibacterium* (phylum *Synergistetes* and *Tannerella (*phylum *Bacteroidetes)* were abundant in peri-implantitis and were present at a higher relative abundance than those found in the H group ($p<0.05$, FDR-adjusted). In contrast, *Streptococcus (*phylum *Firmicutes), Veillonella (*phylum *Firmicutes), Rothia* (phylum *Actinobacteria*) and *Haemophilus* (phylum *Proteobacteria)* had higher relative abundance in H sites ($p<0.05$, FDR-adjusted) (Fig. 1b). Peri-implantitis sites harbored higher levels of classic pathogens (Fig. 1c), such as *Tannerella forsythia*, *Treponema denticola* and *Porphyromonas gingivalis* ($p<0.05$, FDR-adjusted), as well as recently described new putative pathogens, such as *Filifactor alocis, Fretibacterium fastidiosum* and *Treponema maltophilum.* Implants adjacent to H sites were enriched for *Rothia dentocariosa* (Fig.1c).

Analysis of the relative abundance of pathogenic and health-compatible species in individual implants (Fig. 2 a-c) showed that red complex species (*T. forsythia*, *P. gingivalis* and *T. denticola*) were present at high levels in most P samples compared to H samples (Fig. 2a), whereas the opposite was observed for species considered compatible with periodontal/peri-implant health, such as *R. dentocariosa, Streptococcus sanguinis* and *Veillonella dispar* (Fig. 2b). Furthermore, newly proposed periodontal pathogens, such as *F. alocis, F. fastidiosum, Eubacterium saphenum* and *T. maltophilum* and as-of-yet uncultured taxa *Desulfobulbus* sp ot 041, *Fretibacterium sp ot* 360 and *Peptostreptococcacea* sp ot 091 and 369 (Fig. 2c) followed a colonization pattern similar to that of well-recognized periodontal pathogens (*T. forsythia, P. gingivalis* and *T. denticola)* (Fig. 2b).

Next, we employed PCoA to assess the impact of peri-implant health and disease on the local microbiome. A clear distinction between the microbial composition of H and P implants at all taxonomic levels was observed (Fig. 3a-c). Even though it was not the primary objective of the present study, we also explored the potential impact of smoking status and implant system used on the peri-implant microbiome. When the smoking status was incorporated in the analysis (Fig. 3b), it became apparent that the composition of the microbiome of current smokers in the H microbiome was closer to that of peri-implantitis cases than to that observed in successful implants. The impact of the implant system on the local microbiome seemed to be less evident (Fig. 3c).

Because our results indicated that smoking and implant type could be possible confounders when the microbiome of peri-implant health and disease was compared, potential interactions between these parameters were also included in our statistical model. The results revealed an interaction between smoking and disease status for *T. socranskii* and *Eubacterium saphenum*, interactions

between smoking and implant type for *T. maltophilum* and *E. saphenum*, and interactions between disease status and implant type for *T. maltophilum*.

The commensal and pathogenic microbial profiles of H and P groups became clearer with the analysis of the peri-implant core microbiome (Fig. 4). Taxa typically known as host-compatible, such as *Veilonella parvula, S. sanguinis* and *Rothia* sp. were part of the peri-implant health core, while the red complex species *(T. forsythia, P. gingivalis* and *T. denticola)*, as well as "new putative pathogens" *Filifactor alocis, Treponema maltophilum* and *Fretibacterium_fastidiosum* comprised the peri-implantitis core.

The use of HOMI*NGS* complemented the QIIME data, as it allowed for the species-level analysis of taxa that could not be "speciated" by QIIME. For instance, QIIME identified additional taxa from the genus *Porphyromonas* (Group_4) in the peri-implantitis core whereas HOMINGS classified some of them as *Porphyromonas endodontalis.* Similarly, it identified *Campylobacter gracilis* and *Veillonella dispar* as members of the same core, while QIIME indicated the presence of members of the genera *Campylobacter* (*phylum Proteobacteria)* and *Veillonella* (Fig. 4, Supplemental Fig. 2).

Because HOMI*NGS* is a new bioinformatics approach for the analysis of sequencing data, we compared its results with those obtained with QIIME, a more established pipeline. Since QIIME does not allow complete species-level taxonomic resolution, genus-level comparisons were made. Results were quite comparable and most taxa that differed between peri-implant health and disease reported in Fig. 1a-c were also observed in the QIIME pipeline (Supplementary Fig. 3a-c, Supplemental Table 2).

Discussion

The use of next generation sequencing to explore the microbiome of healthy and diseased peri-implant sites allowed us to expand the breadth of knowledge of the etiology of this disease. We used QIIME and HOMI*NGS* to analyze Illumina MiSeq-generated reads and demonstrated that QIIME and HOMI*NGS* agreed in large part at the genus level (Supplemental Table 2). We showed that those pipelines should be complementary: to a certain extent QIIME provided greater breadth of classification whereas HOMI*NGS* provided increased precision. We propose that using two accepted and complementary techniques will shed more light on a difficult (and somewhat ill-defined) classification.

In the present study, we were able to determine major microbial differences between peri-implant healthy and diseased sites and delineate the core microbiome of peri-implant health and peri-implantitis. The microbial differences between the two clinical groups were clear at all taxonomic levels. Peri-implantitis sites harbored greater levels of members of the phyla *Bacteroidetes*, *Spirochetes*, *Synergistetes* and *Tenericutes*, as well as taxa from the genera *Porphyromonas*, *Treponema*, *Filifactor* and *Fretibacterium*. Using fluorescence *in situ* hybridization (FISH) combined with epifluorescence microscopy to analyze samples from the same individuals, Belibasakis and co-workers (Belibasakis et al., 2016) also found elevated levels of *Synergistetes* and *Spirochetes* in peri-implantitis sites. Furthermore, diseased sites were heavily colonized by traditional pathogens, such as red complex species, as well as newly proposed pathogenic taxa (Perez-Chaparro et al., 2014), such as *F. alocis*, *F. fastidiosum* and *Desulfobulbus* sp. oral taxon 041, which is currently uncultured. Conversely, *Streptococci* were highly abundant in healthy implants. Our findings corroborate previous studies suggesting similarities between peri-implant associated microbiota and the periodontal microbiota. Using

checkerboard DNA-DNA hybridization, (Shibli et al., 2008) found high mean counts of all red complex species in peri-implantitis samples, while host-compatible microorganisms were reduced. Our results are also in line with early cloning and sequencing studies of the peri-implant microbiome, in which *Porphyromonas*, *Fusobacterium* and *Filifactor* species were abundant (da Silva et al., 2014, Koyanagi et al., 2013).

Several of the traditional pathogens as well as newly proposed pathogenic taxa were detected in overall low mean relative abundance levels in our study (Fig. 1c, 2a, 2c). Albeit, similar to levels reported by others (Maruyama et al., 2014), the pathogenic capacity of low level taxa might be intriguing. However, it is well-accepted that the presence of taxa in low abundance does not deny their potential importance. In fact, that is the tenet of the keystone-pathogen hypothesis, which holds that "certain low-abundance microbial pathogens can orchestrate inflammatory disease by remodeling a benign microbiota into a dysbiotic one" (Hajishengallis & Lambris, 2012).

In our peri-implantitis samples, we could not confirm reports of the presence of bacteria typically detected in infections of implanted medical devices (Mombelli & Decaillet, 2011) or species not traditionally associated with periodontitis, including *Helicobacter pylori*, *Staphylococcus aureus* and *Staphylococcus anaerobius* (Persson & Renvert, 2014), although *H. influenza* was part of the peri-implant core microbiome. Our results are also in contrast with those of (Kumar et al., 2012). Using pyrosequencing, the authors found that peri-implantitis harbored lower levels of *Prevotella* and *Leptotrichia* and higher levels of *Actinomyces*, *Peptococcus*, *Campylobacter*, non-mutans *Streptococcus*, *Butyrivibrio* and *Streptococcus mutans* than healthy implants. A subsequent paper from the same group (Dabdoub et al., 2013) reported that *Staphylococcus* was significantly associated with implant infection and that red complex pathogens were found in only 37 % of the peri-implantitis biofilms.

The discrepancies presented above may be, in part, due to the use of distinct sample collection methods. While in our study we employed curettes, several publications on the peri-implant microbiome have used paper points (Dabdoub et al. 2013, Tsigarida et al. 2015). However, this method has been demonstrated to harbor DNA of its own (van der Horst et al., 2013), which can alter the representation of the microbiome under study, particularly when sensitive sequencing platforms are used. Thus, their use has been discouraged, in favor of curettes (van der Horst et al., 2013). The above discrepancies may also be due to differences in sequencing platforms and bioinformatics pipelines. MiSeq Illumina sequencing has recently outperformed pyrosequencing, allowing an inexpensive and deeper coverage of the microbiome (Caporaso et al., 2012, Frey et al., 2014, Nelson et al., 2014, Smith & Peay, 2014). MiSeq technology has a lower error rate compared to pyrosequencing and generates over 10 times as many reads as 454 GS FLX (Nelson et al., 2014). Thus, it has become the leading sequencing platform, particularly for human microbiome sequencing studies (Amarasekara et al., 2015). Furthermore, since our goal was to define a core microbiome commonly present on implants, and those frequently associated with peri-implant health or disease only, we used a very conservative approach to assign taxa as present in our samples. For instance, taxa were removed from consideration if they did not have at least 3 reads in at least 3 samples in both the healthy and peri-implantitis groups after rarefication. The goal was to "weed out" species belonging to the so-called "rare biosphere". The idea of determining taxa consistently found in human disease conditions or in specific environments, the so-called core microbiome, has been adopted by many in microbial ecology (Human Microbiome Project Consortium 2012, Backhed et al., 2012, Shade & Handelsman, 2012). The use of this approach might have also contributed to differences between our results and those from previous studies.

While the healthy and peri-implantitis cores were rich in health-compatible and pathogenic taxa, respectively, we observed that the peri-implant microbiome core contained members of genera *Fusobacterium, Parvimonas* and *Campylobacter*. Interestingly, those genera harbor species known to be associated with periodontal inflammation (Socransky & Haffajee, 2005), such as *F. nucleatum, P. micra* and *C. rectus,* all of which are members of the orange complex. Hence, it is plausible that implants are colonized by bacterial species that predispose the adjacent tissues to inflammation.

In order obtain species-level taxonomic resolution from MiSeq sequencing, we employed HOMI*NGS,* an *in silico* 16S rDNA probe analysis that allows the identification of more than 600 oral bacterial species/phylotypes from MiSeq-generated reads (Belstrom et al., 2016a, Belstrom et al., 2016d). HOMI*NGS* has been validated and has been increasingly used in oral microbiology studies (Gomes et al., 2015, McIntyre et al., 2016, Mougeot et al., 2017, Mougeot et al., 2016, Rudney et al., 2015, Timby et al., 2017, Belstrom et al., 2016a, Belstrom et al., 2016b, Belstrom et al., 2016c, Belstrom et al., 2016d, Belstrom et al., 2017). Yet, due to the novelty of the use of HOMI*NGS*, we validated our findings by comparing QIIME and HOMI*NGS* genus-level data (Supplemental Table 2). The results were quite consistent, indicating the robustness of our analytical pipelines, and the validity of the HOMI*NGS* technique.

The combination of these approaches allowed us to detect newly proposed pathogens, such as *P. endododontalis*, *F. alocis* and *F. fastidiosum* and *Desulfobulbus* sp oral taxon 041, all with significant virulence properties. *P. endodontalis* can induce osteoclastogenesis (Ma et al., 2017, Yu et al., 2015), *F. alocis* and *P. endodontalis* present robust NOD1 and NOD2 stimulatory activity, respectively (Marchesan et al., 2016) and *F. alocis* has oxidative stress resistance,

neutrophil and macrophage evasion, adhesion and invasion among its main virulence factors (Aruni et al., 2014). In addition, transcriptional activity analysis of the periodontal microbiome and the human host in health and chronic periodontitis showed that the upregulation of bacterial chemotaxis, flagellar assembly, type III secretion system, and type III CRISPR-Cas system was driven not only by the red-complex pathogens, but also by candidate pathogens, including *F. alocis* and *F. fastidiosum* (Deng et al., 2017). Finally, our results suggest that phylotypes, such as Desulfobulbus sp HOT 041, might also contribute to the development of peri-implantitis. Culture-independent studies have demonstrated the association of this phylotype with periodontitis (Camelo-Castillo et al., 2015, Oliveira et al., 2016), however information on its virulence properties is scarce due to its status of "as-of-yet uncultured organism". Still, the isolation and sequencing of single cells of oral *Desulfobulbus* (n=7) identified genes associated with several categories of putative virulence factors, including chemotaxis, flagellum biosynthesis motor proteins secretion, iron acquisition, stress response, evasion, proteases, and adhesion. Collectively, these findings support the pathogenic role of newly identified pathogens and that they merit further examination of their potential role as etiologic agents of peri-implantitis.

The peri-implantitis group included more smokers than the peri-implant healthy group, which is in line with the literature, as smoking is a well-known risk factor for peri-implantitis (Heitz-Mayfield, 2008). Part of the deleterious effects of smoking on implant survival might be due to its impact on the peri-implant microbiota. As demonstrated by (Tsigarida et al., 2015), smoking shapes the peri-implant microbiome even in clinical health, promoting a pathogen-rich community depleted of commensals. This phenomenon was also observed in the present study, where healthy implants from non-smokers had microbial profiles distinct from those found in

current smokers, which appeared to be more similar to a peri-implantitis microbiome (Fig. 3 a-c). This finding could help justify the differences in the core microbiomes in peri-implant health and disease. To examine this possibility, our statistical models tested for interactions between smoking and disease status. We only found interactions between smoking and disease status for *T. socranskii* and *E. saphenum*, thereby supporting the notion that the main driver of differences in the core microbiome between peri-implant health and peri-implantitis was the disease status.

Due to the scarce literature on the comparison of the microbiomes of different implant systems, we also explored their impact on the local microbiome. Straumann implants were the most frequently used in both groups (Table 1), but the implant system did not modulate the microbial composition of peri-implant biofilms (Fig. 3 b-c).

Although it was not our goal to compare the peri-implant and periodontal microbiota, our results support the notion that both are similar. Using pyrosequencing, Maruyama and co-workers (Maruyama et al., 2014) performed this comparison and concluded that the core microbiome associated with these clinical conditions differed, and suggested that they presented "different causative pathogens". However, only *Prevotella nigrescens* had significantly higher relative abundance in peri-implantitis compared to periodontitis, while *Peptostreptococcaceae* [XI] [G-4], sp. HOT369 and *Desulfomicrobium orale* were more abundant in periodontitis. Furthermore, their PCoA did not demonstrate that the two diseases differed in their community structure. Measures of biodiversity were also similar in peri-implantitis and periodontitis. Our results were in accordance with theirs that reported that *P. gingivalis*, *T. denticola* and *T. socranskii* were abundant and prevalent in most samples of peri-implantitis.

The present study suggests that the peri-implant microbiome is quite distinct in health and disease. Peri-implantitis sites showed an enrichment for pathogens, at the expense of a depletion of host-compatible species. Well-recognized periodontal pathogens as well as newly proposed pathogenic taxa, several of which have not yet been cultivated, were associated with peri-implant disease sites. The core peri-implant microbiome contained members of genera *Fusobacterium, Parvimonas* and *Campylobacter sp.,* potentially including pathogenic species such a*s F. nucleatum, P. micra* and *C. rectus*. Our findings are clinically relevant, in that based on these results, it can be postulated that close surveillance, periodic maintenance as well as early diagnosis of peri-implantitis and immediate intervention are critical for the long-term retention of implants

Acknowledgements

This study was supported in part by an ITI Fellowship (to I.S.M.), by the National Institutes of Health/National Institute of Dental and Craniofacial Research (R03-DE021742 and R01-DE024767 to F.R.F.T.) and by a pilot grant from Forsyth's Center for Discovery at the Host-Biofilm Interface (to F.R.F.T). We thank the members of the Forsyth Institute Sequencing Core - Bruce Paster, Jon Mcafferty, Keerthana Krishnan, Sean Cotton and George Chen - for their technical assistance. We also thank Dr. Paul Levi for his assistance and support in the initiation of this project and Dr. Jeff Roach for his technical assistance.

References

Human Microbiome Project Consortium 2012. Structure, function and diversity of the healthy human microbiome. *Nature,* 486**,** 207-14.

Abusleme, L., Dupuy, A. K., Dutzan, N., Silva, N., Burleson, J. A., Strausbaugh, L. D., Gamonal, J. & Diaz, P. I. 2013. The subgingival microbiome in health and periodontitis and its relationship with community biomass and inflammation. *ISME J,* 7**,** 1016-25.

Amarasekara, R., Jayasekara, R. W., Senanayake, H. & Dissanayake, V. H. 2015. Microbiome of the placenta in pre-eclampsia supports the role of bacteria in the multifactorial cause of pre-eclampsia. *J Obstet Gynaecol Res,* 41**,** 662-9.

Aruni, A. W., Zhang, K., Dou, Y. & Fletcher, H. 2014. Proteome analysis of coinfection of epithelial cells with Filifactor alocis and Porphyromonas gingivalis shows modulation of pathogen and host regulatory pathways. *Infect Immun,* 82**,** 3261-74.

Backhed, F., Fraser, C. M., Ringel, Y., Sanders, M. E., Sartor, R. B., Sherman, P. M., Versalovic, J., Young, V. & Finlay, B. B. 2012. Defining a healthy human gut microbiome: current concepts, future directions, and clinical applications. *Cell Host Microbe,* 12**,** 611-22.

Baker, G. C., Smith, J. J. & Cowan, D. A. 2003. Review and re-analysis of domain-specific 16S primers. *J Microbiol Methods,* 55**,** 541-55.

Belibasakis, G. N., Mir-Mari, J., Sahrmann, P., Sanz-Martin, I., Schmidlin, P. R. & Jung, R. E. 2016. Clinical association of Spirochaetes and Synergistetes with peri-implantitis. *Clin Oral Implants Res,* 27**,** 656-61.

Belstrom, D., Holmstrup, P., Bardow, A., Kokaras, A., Fiehn, N. E. & Paster, B. J. 2016a. Comparative analysis of bacterial profiles in unstimulated and stimulated saliva samples. *J Oral Microbiol,* 8**,** 30112.

Belstrom, D., Holmstrup, P., Bardow, A., Kokaras, A., Fiehn, N. E. & Paster, B. J. 2016b. Temporal Stability of the Salivary Microbiota in Oral Health. *PLoS One,* 11**,** e0147472.

Belstrom, D., Holmstrup, P., Fiehn, N. E., Kirkby, N., Kokaras, A., Paster, B. J. & Bardow, A. 2017. Salivary microbiota in individuals with different levels of caries experience. *J Oral Microbiol,* 9**,** 1270614.

Belstrom, D., Holmstrup, P., Fiehn, N. E., Rosing, K., Bardow, A., Paster, B. J. & Lynge Pedersen, A. M. 2016c. Bacterial composition in whole saliva from patients with severe hyposalivation--a case-control study. *Oral Dis,* 22**,** 330-7.

Belstrom, D., Paster, B. J., Fiehn, N. E., Bardow, A. & Holmstrup, P. 2016d. Salivary bacterial fingerprints of established oral disease revealed by the Human Oral Microbe Identification using Next Generation Sequencing (HOMINGS) technique. *J Oral Microbiol,* 8**,** 30170.

Camelo-Castillo, A., Novoa, L., Balsa-Castro, C., Blanco, J., Mira, A. & Tomas, I. 2015. Relationship between periodontitis-associated subgingival microbiota and clinical inflammation by 16S pyrosequencing. *J Clin Periodontol,* 42**,** 1074-82.

Caporaso, J. G., Lauber, C. L., Walters, W. A., Berg-Lyons, D., Huntley, J., Fierer, N., Owens, S. M., Betley, J., Fraser, L., Bauer, M., Gormley, N., Gilbert, J. A., Smith, G. & Knight, R. 2012. Ultra-high-throughput microbial community analysis on the Illumina HiSeq and MiSeq platforms. *ISME J,* 6**,** 1621-4.

Caporaso, J. G., Lauber, C. L., Walters, W. A., Berg-Lyons, D., Lozupone, C. A., Turnbaugh, P. J., Fierer, N. & Knight, R. 2011. Global patterns of 16S rRNA diversity at a depth of millions of sequences per sample. *Proc Natl Acad Sci U S A,* 108 Suppl 1**,** 4516-22.

Carcuac, O., Derks, J., Charalampakis, G., Abrahamsson, I., Wennstrom, J. & Berglundh, T. 2016. Adjunctive Systemic and Local Antimicrobial Therapy in the Surgical Treatment of Peri-implantitis: A Randomized Controlled Clinical Trial. *J Dent Res,* 95**,** 50-7.

Chakravorty, S., Helb, D., Burday, M., Connell, N. & Alland, D. 2007. A detailed analysis of 16S ribosomal RNA gene segments for the diagnosis of pathogenic bacteria. *J Microbiol Methods,* 69**,** 330-9.

Charalampakis, G. & Belibasakis, G. N. 2015. Microbiome of peri-implant infections: lessons from conventional, molecular and metagenomic analyses. *Virulence,* 6**,** 183-7.

Da Silva, E. S., Feres, M., Figueiredo, L. C., Shibli, J. A., Ramiro, F. S. & Faveri, M. 2014. Microbiological diversity of peri-implantitis biofilm by Sanger sequencing. *Clin Oral Implants Res,* 25**,** 1192-9.

Dabdoub, S. M., Tsigarida, A. A. & Kumar, P. S. 2013. Patient-specific analysis of periodontal and peri-implant microbiomes. *J Dent Res,* 92**,** 168S-75S.

Deng, Z. L., Szafranski, S. P., Jarek, M., Bhuju, S. & Wagner-Dobler, I. 2017. Dysbiosis in chronic periodontitis: Key microbial players and interactions with the human host. *Sci Rep,* 7**,** 3703.

Derks, J., Schaller, D., Hakansson, J., Wennstrom, J. L., Tomasi, C. & Berglundh, T. 2016a. Effectiveness of Implant Therapy Analyzed in a Swedish Population: Prevalence of Peri-implantitis. *J Dent Res,* 95**,** 43-9.

Derks, J., Schaller, D., Hakansson, J., Wennstrom, J. L., Tomasi, C. & Berglundh, T. 2016b. Peri-implantitis - onset and pattern of progression. *J Clin Periodontol,* 43**,** 383-8.

Derks, J. & Tomasi, C. 2014. Peri-implant health and disease. A systematic review of current epidemiology. *J Clin Periodontol*.

Derks, J. & Tomasi, C. 2015. Peri-implant health and disease. A systematic review of current epidemiology. *J Clin Periodontol,* 42 Suppl 16**,** S158-71.

Frey, K. G., Herrera-Galeano, J. E., Redden, C. L., Luu, T. V., Servetas, S. L., Mateczun, A. J., Mokashi, V. P. & Bishop-Lilly, K. A. 2014. Comparison of three next-generation sequencing platforms for metagenomic sequencing and identification of pathogens in blood. *BMC Genomics,* 15**,** 96.

Gomes, B. P., Berber, V. B., Kokaras, A. S., Chen, T. & Paster, B. J. 2015. Microbiomes of Endodontic-Periodontal Lesions before and after Chemomechanical Preparation. *J Endod,* 41**,** 1975-84.

Hajishengallis, G. & Lambris, J. D. 2012. Complement and dysbiosis in periodontal disease. *Immunobiology,* 217**,** 1111-6.

Heitz-Mayfield, L. J. 2008. Peri-implant diseases: diagnosis and risk indicators. *J Clin Periodontol,* 35**,** 292-304.

Koyanagi, T., Sakamoto, M., Takeuchi, Y., Maruyama, N., Ohkuma, M. & Izumi, Y. 2013. Comprehensive microbiological findings in peri-implantitis and periodontitis. *J Clin Periodontol,* 40**,** 218-26.

Kumar, P. S., Mason, M. R., Brooker, M. R. & O'brien, K. 2012. Pyrosequencing reveals unique microbial signatures associated with healthy and failing dental implants. *J Clin Periodontol,* 39**,** 425-33.

Ma, N., Yang, D., Okamura, H., Teramachi, J., Hasegawa, T., Qiu, L. & Haneji, T. 2017. Involvement of interleukin23 induced by Porphyromonas endodontalis lipopolysaccharide in osteoclastogenesis. *Mol Med Rep,* 15**,** 559-566.

Marchesan, J., Jiao, Y. Z., Schaff, R. A., Hao, J., Morelli, T., Kinney, J. S., Gerow, E., Sheridan, R., Rodrigues, V., Paster, B. J., Inohara, N. & Giannobile, W. V. 2016. TLR4, NOD1 and NOD2 mediate immune recognition of putative newly identified periodontal pathogens. *Mol Oral Microbiol,* 31**,** 243-58.

Maruyama, N., Maruyama, F., Takeuchi, Y., Aikawa, C., Izumi, Y. & Nakagawa, I. 2014. Intraindividual variation in core microbiota in peri-implantitis and periodontitis. *Sci Rep,* 4**,** 6602.

Mcintyre, M. K., Peacock, T. J., Akers, K. S. & Burmeister, D. M. 2016. Initial Characterization of the Pig Skin Bacteriome and Its Effect on In Vitro Models of Wound Healing. *PLoS One,* 11**,** e0166176.

Mombelli, A. & Decaillet, F. 2011. The characteristics of biofilms in peri-implant disease. *J Clin Periodontol,* 38 Suppl 11**,** 203-13.

Mombelli, A., Muller, N. & Cionca, N. 2012. The epidemiology of peri-implantitis. *Clin Oral Implants Res,* 23 Suppl 6**,** 67-76.

Moraschini, V., Poubel, L. A., Ferreira, V. F. & Barboza Edos, S. 2015. Evaluation of survival and success rates of dental implants reported in longitudinal studies with a follow-up period of at least 10 years: a systematic review. *Int J Oral Maxillofac Surg,* 44**,** 377-88.

Mougeot, J. C., Stevens, C. B., Paster, B. J., Brennan, M. T., Lockhart, P. B. & Mougeot, F. K. 2017. Porphyromonas gingivalis is the most abundant species detected in coronary and femoral arteries. *J Oral Microbiol,* 9**,** 1281562.

Mougeot, J. L., Stevens, C. B., Cotton, S. L., Morton, D. S., Krishnan, K., Brennan, M. T., Lockhart, P. B., Paster, B. J. & Bahrani Mougeot, F. K. 2016. Concordance of HOMIM and HOMINGS technologies in the microbiome analysis of clinical samples. *J Oral Microbiol,* 8**,** 30379.

Nelson, M. C., Morrison, H. G., Benjamino, J., Grim, S. L. & Graf, J. 2014. Analysis, optimization and verification of Illumina-generated 16S rRNA gene amplicon surveys. *PLoS One,* 9**,** e94249.

Oliveira, R. R., Fermiano, D., Feres, M., Figueiredo, L. C., Teles, F. R., Soares, G. M. & Faveri, M. 2016. Levels of Candidate Periodontal Pathogens in Subgingival Biofilm. *J Dent Res,* 95**,** 711-8.

Ong, S. H., Kukkillaya, V. U., Wilm, A., Lay, C., Ho, E. X., Low, L., Hibberd, M. L. & Nagarajan, N. 2013. Species identification and profiling of complex microbial communities using shotgun Illumina sequencing of 16S rRNA amplicon sequences. *PLoS One,* 8**,** e60811.

Pei, A. Y., Oberdorf, W. E., Nossa, C. W., Agarwal, A., Chokshi, P., Gerz, E. A., Jin, Z., Lee, P., Yang, L., Poles, M., Brown, S. M., Sotero, S., Desantis, T., Brodie, E., Nelson, K. & Pei, Z. 2010. Diversity of 16S rRNA genes within individual prokaryotic genomes. *Appl Environ Microbiol,* 76**,** 3886-97.

Perez-Chaparro, P. J., Goncalves, C., Figueiredo, L. C., Faveri, M., Lobao, E., Tamashiro, N., Duarte, P. & Feres, M. 2014. Newly identified pathogens associated with periodontitis: a systematic review. *J Dent Res,* 93**,** 846-58.

Persson, G. R. & Renvert, S. 2014. Cluster of bacteria associated with peri-implantitis. *Clin Implant Dent Relat Res,* 16**,** 783-93.

Rudney, J. D., Jagtap, P. D., Reilly, C. S., Chen, R., Markowski, T. W., Higgins, L., Johnson, J. E. & Griffin, T. J. 2015. Protein relative abundance patterns associated with sucrose-induced dysbiosis are conserved across taxonomically diverse oral microcosm biofilm models of dental caries. *Microbiome,* 3**,** 69.

Shade, A. & Handelsman, J. 2012. Beyond the Venn diagram: the hunt for a core microbiome. *Environ Microbiol,* 14**,** 4-12.

Shibli, J. A., Melo, L., Ferrari, D. S., Figueiredo, L. C., Faveri, M. & Feres, M. 2008. Composition of supra- and subgingival biofilm of subjects with healthy and diseased implants. *Clin Oral Implants Res,* 19**,** 975-82.

Smith, D. P. & Peay, K. G. 2014. Sequence depth, not PCR replication, improves ecological inference from next generation DNA sequencing. *PLoS One,* 9**,** e90234.

Socransky, S. S. & Haffajee, A. D. 2005. Periodontal microbial ecology. *Periodontol 2000,* 38**,** 135-87.

Teles, R. P., Bogren, A., Patel, M., Wennstrom, J. L., Socransky, S. S. & Haffajee, A. D. 2007. A three-year prospective study of adult subjects with gingivitis II: microbiological parameters. *J Clin Periodontol,* 34**,** 7-17.

Timby, N., Domellof, M., Holgerson, P. L., West, C. E., Lonnerdal, B., Hernell, O. & Johansson, I. 2017. Oral Microbiota in Infants Fed a Formula Supplemented with Bovine Milk Fat Globule Membranes - A Randomized Controlled Trial. *PLoS One,* 12**,** e0169831.

Tsigarida, A. A., Dabdoub, S. M., Nagaraja, H. N. & Kumar, P. S. 2015. The Influence of Smoking on the Peri-Implant Microbiome. *J Dent Res,* 94**,** 1202-17.

Van Der Horst, J., Buijs, M. J., Laine, M. L., Wismeijer, D., Loos, B. G., Crielaard, W. & Zaura, E. 2013. Sterile paper points as a bacterial DNA-contamination source in microbiome profiles of clinical samples. *J Dent,* 41**,** 1297-301.

Vigolo, P., Mutinelli, S., Zaccaria, M. & Stellini, E. 2015. Clinical evaluation of marginal bone level change around multiple adjacent implants restored with splinted and nonsplinted restorations: a 10-year randomized controlled trial. *Int J Oral Maxillofac Implants,* 30**,** 411-8.

Wang, Y. & Qian, P. Y. 2009. Conservative fragments in bacterial 16S rRNA genes and primer design for 16S ribosomal DNA amplicons in metagenomic studies. *PLoS One,* 4**,** e7401.

Yu, Y., Qiu, L., Guo, J., Yang, D., Qu, L., Yu, J., Zhan, F., Xue, M. & Zhong, M. 2015. TRIB3 mediates the expression of Wnt5a and activation of nuclear factor-kappaB in Porphyromonas endodontalis lipopolysaccharide-treated osteoblasts. *Mol Oral Microbiol,* 30**,** 295-306.

Zitzmann, N. U. & Berglundh, T. 2008. Definition and prevalence of peri-implant diseases. *J Clin Periodontol,* 35**,** 286-91.

FIGURE LEGENDS

Figure 1. Box plots of differences in microbial relative abundance between samples from healthy and peri-implantitis (disease) sites at the level of phylum (a), genus (b), and species (c). Phylum-, genus- and species-level data were obtained using HOMI*NGS*. Taxa were sorted according to decreasing relative abundance in subjects with peri-implantitis. Only taxa that were significantly different between the healthy and peri-implantitis groups (with FDR-adjusted p-values <0.05) in more than 95% of the 100 iterations performed were plotted.

Figure 2. Relative abundance of pathogenic and health-compatible species in individual implants. Graphs show mean relative abundance (%) for (a) well-recognized periodontal pathogens, (b) putative commensals and (c) newly proposed pathogenic taxa. Only species that were significantly different between the healthy and peri-implantitis groups (with FDR-adjusted p-values <0.05) in more than 98% of the 100 iterations performed were plotted. Each bar represents one individual healthy (blue) or diseased (red) implant.

Figure 3. **Principal Coordinate Analysis (PCoA) of the microbial composition of samples according to disease status (a), smoking habit (b) and brand of implant (c)**. Graphs represent the PCoA plots of Bray–Curtis distances based on species level data generated with HOMI*NGS*. Samples from subjects presenting healthy (blue) and diseased (red) peri-implant sites (a) are plotted according to smoking habit (b) and type of implant (c).

Figure 4. Core Microbiome. Taxa that were present with ≥ 0.1% relative abundance in ≥ 50% of all samples according to HOMI*NGS* results constitute the core microbiome (blue). Samples were divided into those representing healthy or peri-implantitis. The core microbiome was subdivided into 4 groups based on the mean relative abundance of the taxa in samples in each clinical category. Taxa that were present in ≥ 50% of samples in a single category, but were not part of the core microbiome considering all samples, constituted the Healthy (green) or Peri-implantitis (red) core microbiomes. Taxa in those core microbiomes were sub-grouped based on the mean relative abundance of the taxa in samples in each clinical group. Taxa in bold were present in ≥ 75% of all samples (Core).

Supplemental Figure 1. Alpha and Beta Diversity. a) Measure of alpha diversity in healthy and peri-implantitis sites as determined by the Chao 1 index. b) Beta diversity represented by Principal Component Analysis plots of unweighted Unifrac distances.

Supplemental Figure 2. Core Microbiome. Taxa that were present with ≥ 0.1% relative abundance in ≥ 50% of all samples according to QIIME results constitute the Core Microbiome (blue). Samples were divided into those representing healthy or peri-implantitis. The Core Microbiome was subdivided into 4 groups based on the mean relative abundance of the taxa in samples in each clinical category. Taxa that were present in ≥ 50% of samples in a single category, but were not part of the Core Microbiome considering all samples, constitute the Healthy (green) or Per-iimplantitis (red) Core Microbiomes. Taxa in those Core Microbiomes were sub-grouped based on the mean relative abundance of the taxa in samples in each clinical

group. Taxa in bold were present in ≥ 75% of all samples (Core). Taxa that could not be resolved to the species-level are presented as groups, described as follows:

1. Parvimonas_Group_16: Parvimonas_micra, sp_oral_taxon_110, sp_oral_taxon_393
2. Treponema_Group_27: Treponema_socranskii, sp_oral_taxon_268, sp_oral_taxon_269
3. Veillonella_Group_19: Veillonella_atypica, denticariosi, dispar, parvula
4. Neisseria_Group_21: Neisseria_flava, mucosa, oralis, pharynges, sicca, sp_oral_taxon_016, sp_oral_taxon_018, subflava
5. Porphyromonas_Group_4: Porphyromonas_endodontalis, sp_oral_taxon_285, sp_oral_taxon_395
6. Fretibacterium_Group_28: Fretibacterium_sp_oral_taxon_358, sp_oral_taxon_359, sp_oral_taxon_360, sp_oral_taxon_361, sp_oral_taxon_362, sp_oral_taxon_452, sp_oral_taxon_453

Supplemental Figure 3. Box plots of differences in microbial relative abundance between samples from healthy and peri-implantitis sites at the level of phylum (a), genus (b), and species (c). Phylum, genus and species-level data were obtained using QIIME. Taxa were sorted according to decreasing relative abundance in subjects with peri-implantitis. Only taxa that were significantly different between the healthy and peri-implantitis groups (with FDR-adjusted p-values < 0.05) in more than 95% of the 100 iterations performed were plotted.

Table 1: Characteristics of the peri-implant sites sampled.

Parameters	Healthy (n = 32)	Peri-implantitis (n = 35)	p-value
Patient age (years ± SD)	57 ± 16	59 ± 14	0.509
Gender (M/F)	10/22	12/23	1
Implant wear (years ± SD)	6.3 ± 4.4	7.3 ± 3.6	0.312
Bone loss (mm ± SD)	0.03 ± 0.18	6.7 ± 2.4	<0.0001
Suppuration at any site (# subjects/total)	0/32	18/35	<0.0001
Suppuration proportion of sites per subject	0	0.35 ± 0.41	<0.0001
PD (average of 6 sites) (mm ± SD)	3.1 ± 0.5	7.0 ± 2.5	<0.0001
PD (at site sampled) (mm ± SD)	3.2 ± 0.7	7.5 ± 3.0	<0.0001
BOP at any site (# subjects/total)	19/32	34/35	0.0002
BOP proportion of sites per subject	24 ± 29	80 ± 26	<0.0001
PI at any site (# subjects/total)	13/32	24/35	0.028
PI proportion of sites per subject	12 ± 19	45 ± 38	<0.0001
Keratinized mucosa (average of 5 sites) (mm ± SD)	3.3 ± 1.5	2.2 ± 1.8	0.009
Keratinized mucosa (at site sampled) (mm ± SD)	3.3 ± 2.1	2.3 ± 2.0	0.034
Location of implant (maxilla/mandible)	16/16	18/17	1
Location of implant (posterior/anterior)	24/8	29/6	0.551
Type of restoration (fixed/removable)	30/2	32/3	1

Smokers (%)			0.033
non-smoker	71.9%	37.1%	
former smoker	3.1%	11.4%	
current smoker	21.9%	42.9%	
missing data	3.1%	8.6%	
Pack years (years ± SD)	29 ± 22 (n=7)	19 ± 14 (n=15)	0.247
Implant System (%)			0.003
Straumann	71.9%	47.1%	
Branemark	25.0%	17.7%	
Other	3.1%	35.3%	

Note: PD=pocket depth, BOP=bleeding on probing, PI=plaque index, SD=standard deviation.

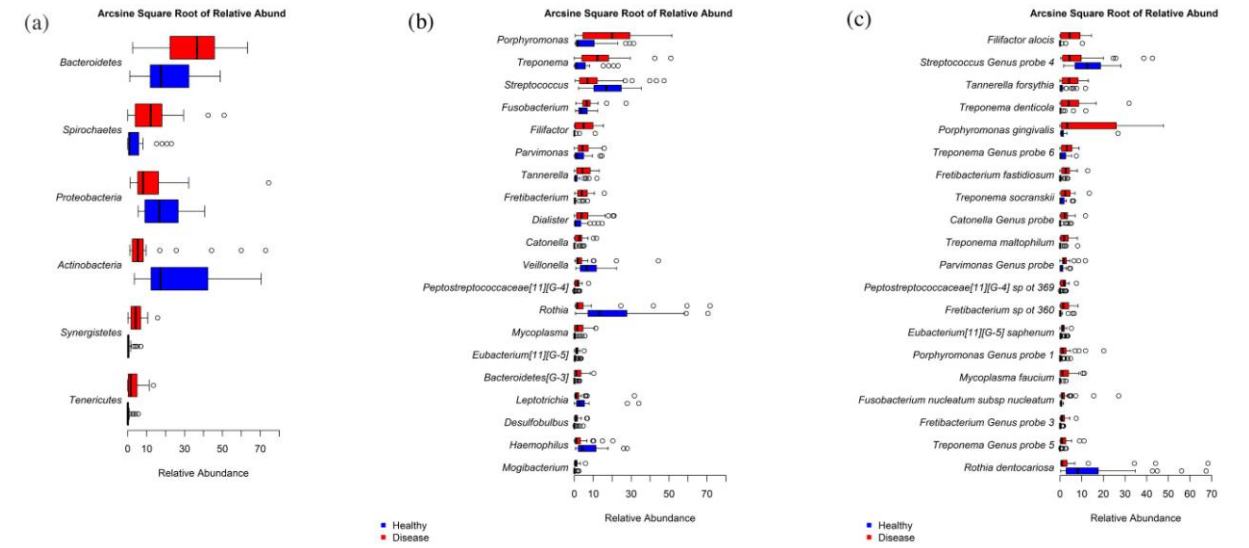
(a)
Arcsine Square Root of Relative Abund
Bacteroidetes
Spirochaetes
Proteobacteria
Actinobacteria
Synergistetes
Tenericutes
0 10 30 50 70
Relative Abundance
(b)
Arcsine Square Root of Relative Abund
Porphyromonas
Treponema
Streptococcus
Fusobacterium
Filifactor
Parvimonas
Tannerella
Fretibacterium
Dialister
Catonella
Veillonella
Peptostreptococcaceae[11][G-4]
Rothia
Mycoplasma
Eubacterium[11][G-5]
Bacteroidetes[G-3]
Leptotrichia
Desulfobulbus
Haemophilus
Mogibacterium
0 10 30 50 70
Relative Abundance
Healthy
Disease
(c)
Arcsine Square Root of Relative Abund
Filifactor alocis
Streptococcus Genus probe 4
Tannerella forsythia
Treponema denticola
Porphyromonas gingivalis
Treponema Genus probe 6
Fretibacterium fastidiosum
Treponema socranskii
Catonella Genus probe
Treponema maltophilum
Parvimonas Genus probe
Peptostreptococcaceae[11][G-4] sp ot 369
Fretibacterium sp ot 360
Eubacterium[11][G-5] saphenum
Porphyromonas Genus probe 1
Mycoplasma faucium
Fusobacterium nucleatum subsp nucleatum
Fretibacterium Genus probe 3
Treponema Genus probe 5
Rothia dentocariosa
0 10 20 30 40 50 60 70
Relative Abundance
Healthy
Disease

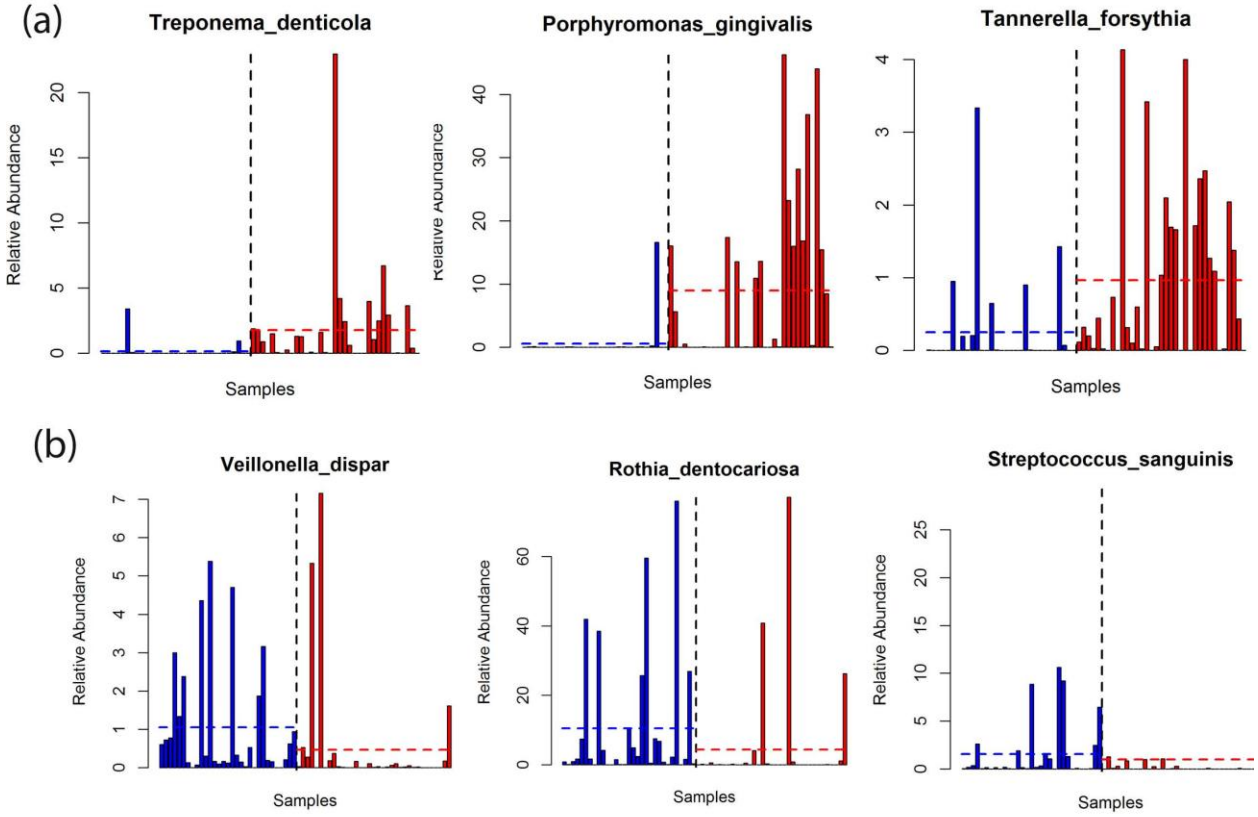
(a)
Treponema_denticola
Porphyromonas_gingivalis
Tannerella_forsythia
Relative Abundance
Samples
(b)
Veillonella_dispar
Rothia_dentocariosa
Streptococcus_sanguinis
Relative Abundance
Samples

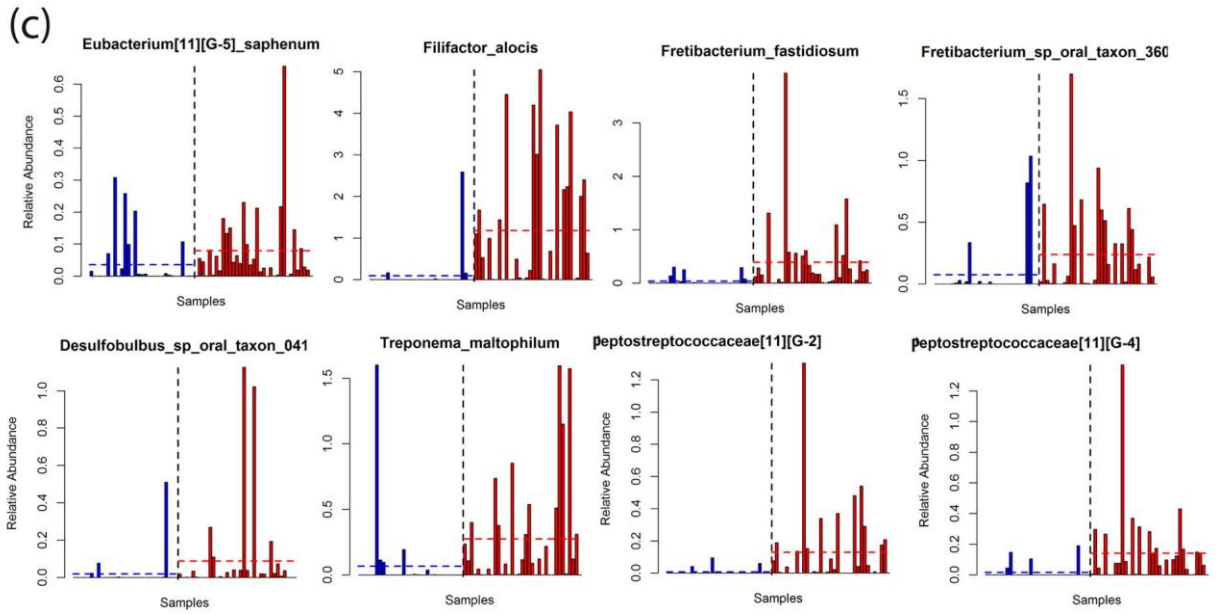
(c)
Eubacterium[11][G-5]_saphenum
Filifactor_alocis
Fretibacterium_fastidiosum
Fretibacterium_sp_oral_taxon_360
Desulfobulbus_sp_oral_taxon_041
Treponema_maltophilum
Peptostreptococcaceae[11][G-2]
Peptostreptococcaceae[11][G-4]
Relative Abundance
Samples

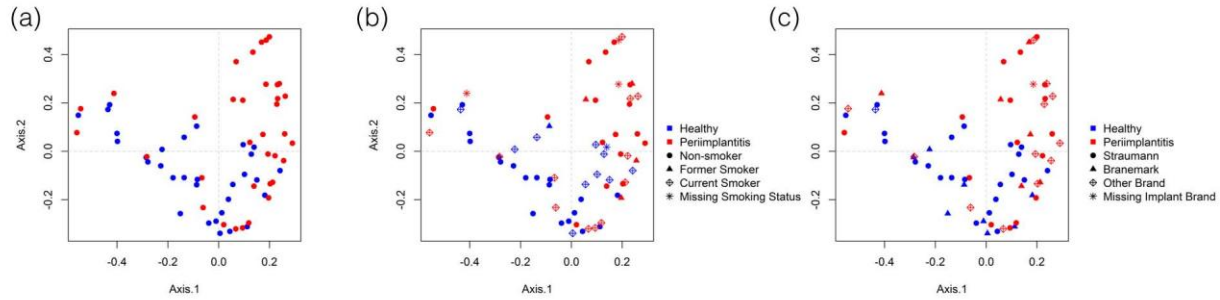
(a)
(b)
(c)
Axis.1
Axis.2
Healthy
Periimplantitis
Non-smoker
Former Smoker
Current Smoker
Missing Smoking Status
Straumann
Branemark
Other Brand
Missing Implant Brand

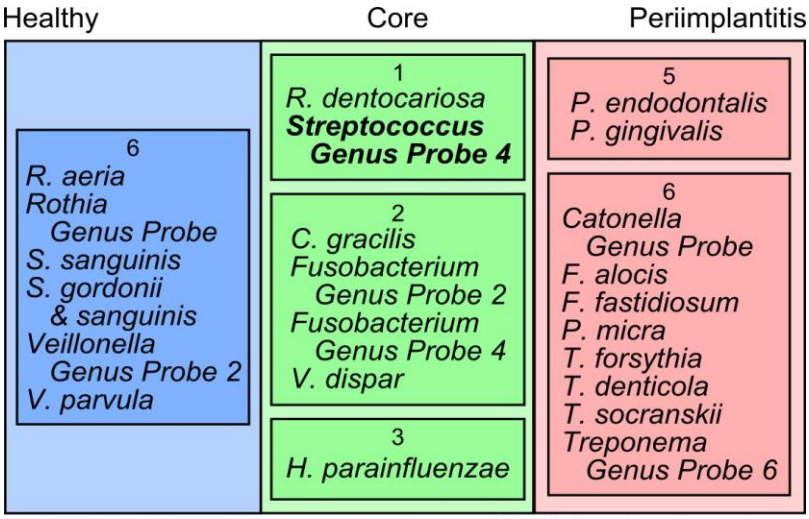

Core Microbiome: Taxa present with >= 0.1% relative abundance in >= 50% of all samples

Healthy Core: Taxa present with >= 0.1% relative abundance in >= 50% of healthy samples, but not in the Core Microbiome

Periimplantitis Core: Taxa present with >= 0.1% relative abundance in >= 50% of periimplantitis samples, but not in the Core Microbiome

Bold: Taxa present with >= 0.1% relative abundance in >= 75% of all samples or samples belonging to the indicated category

1: Mean relative abundance >= 2% in both blue and red categories

2: Mean relative adundance < 2 % in both blue and red categories

3: Mean relative abundance >= 2 % in blue category and < 2% in red category

4: Mean relative abundance < 2% in blue category and >= 2% in red category

5: Mean relative abundance >= 2% for the category

6: Mean relative abundance < 2% for the category

Rothia Genus Probe: aeria, dentocariosa, mucilaginosa

Veillonella Genus Probe 2: sp oral taxon 129, 132, 150, 918

Streptococcus Genus Probe 4: australis, cristatus, infantis, mitis, mitis bv 2, oligofermentans, oralis, parasanguinis, parasanguinis II, peroris, pneumoniae, pseudopneumoniae, salivarius, sinensis, vestibularis, sp oral taxon 055, 056, 057, 058, 061, 064, 065, 066, 067, 068, 069, 070, 071, 074, 423, 431, 486

Fusobacterium Genus Probe 2: naviforme, nucleatum subsp animalis, nucleatum subsp vincentii, sp oral taxon 205

Fusobacterium Genus Probe 4: canifelinum, naviforme necrophorum, nucleatum subsp animalis, nucleatum subsp fusiforme, nucleatum subsp nucleatum, nucleatum subsp polymorphum, nucleatum subsp vincentii, periodonticum, simiae, sp oral taxon_203, 205, 370

Catonella Genus Probe: morbi, sp oral taxon 164, 451

Treponema Genus Probe 6: socranskii subsp buccale, socranskii subsp pedis, socranskii subsp socranskii, sp oral taxon 268, 269